Langmuir
Article
pubs.acs.org/Langmuir

Self-Assembled Monolayers of Alkanethiols on InAs

Dmitri Y. Petrovykh,[*,†,‡,§] Jennifer C. Smith,[‡,§] Thomas D. Clark,[‡] Rory Stine,[‡] Lane A. Baker,[‡,‖]
and Lloyd J. Whitman[‡,⊥]

[†]Physics Department, University of Maryland, College Park, Maryland 20742, and [‡]Naval Research Laboratory, Washington, D.C. 20375. [§]J.C.S. and D.Y.P. contributed equally to this work. [‖] Current address: Department of Chemistry, Indiana University, Bloomington, IN 47405. [⊥] Current address: Center for Nanoscale Science and Technology, National Institute of Standards and Technology, Gaithersburg, MD 20899.

Received December 30, 2008. Revised Manuscript Received September 1, 2009

We describe the deposition and properties of self-assembled monolayers (SAMs) of methyl-terminated alkanethiols on InAs(001) surface. For these model hydrophobic films, we used water contact angle measurements to survey the preparation of alkanethiol monolayers from base-activated ethanolic solutions as a function of the solution and deposition parameters, including chain length of alkanethiols, deposition time, and solution temperature and pH. We then used X-ray photoelectron spectroscopy (XPS), ellipsometry, and electrochemistry to characterize the composition and structure of octadecanethiol (ODT) monolayers deposited on InAs under optimized conditions. When applied to a thoroughly degreased InAs(001) wafer surface, the basic ODT solution removes the native oxide without excessively etching the underlying InAs(001) substrate. The resulting film contains approximately one monolayer of ODT molecules, attached to the InAs surface almost exclusively via thiolate bonds to In atoms, with organic chains extended away from the surface. These ODT monolayers are stable against degradation and oxidation in air, organic solvents, and aqueous buffers. The same base-activated ODT treatment can also be used to passivate exposed InAs/AlSb quantum well (QW) devices, preserving the unique electronic properties of InAs surfaces and allowing the operation of such passivated devices as continuous flow pH-sensors.

1. Introduction

Until recently, self-assembled monolayers (SAMs) on surfaces of III−V semiconductors had remained relatively unexplored, compared to the extensive studies of SAMs on metals[1,2] and Group IV semiconductors.[3] The current interest in SAM formation on III−V semiconductors, including InAs, is motivated by potential applications in microelectronics, nanotechnology, molecular electronics, and sensors.[4−6] Since the pioneering work by Allara et al.,[7] the primary focus has been on the most technologically important III−V semiconductor surface—GaAs(001).[7−16] For In-based III−V materials, alkanethiol SAMs have been prepared and characterized on InP;[17−20] alkanethiol films[21] and monolayers of bifunctional molecules[22] have been examined on InAs.

SAMs can fulfill two important roles on the surfaces of chemical or biological sensors: *passivation* and *functionalization*.[6,23] For sensors, *passivation* means creating surfaces having stable chemical and electronic properties that do not change with exposure to ambient air, aqueous environments, and organic solvents. Such passivation is required because most semiconductor surfaces are chemically reactive and electronically deficient or unstable. *Functionalization* of sensor surfaces involves immobilization of moieties that impart the required sensitivity to chemical or biological targets; functionalization can also include controlling surface properties such as hydrophobicity or charge. In general, any practical treatment of sensor surfaces would benefit from being compatible with wet chemistry and providing a convenient pathway for further modification. SAMs not only readily furnish these desired attributes for a wide variety of functionalized surfaces,[1−3,24,25] but also have proven to be particularly

---

*Author to whom correspondence should be addressed. Address: Code 6176 Naval Research Laboratory, Washington, DC 20375-5342. E-mail: dmitri.petrovykh@nrl.navy.mil

(1) Duwez, A. S. *J. Electron Spectrosc. Relat. Phenom.* **2004**, *134*(2−3), 97–138.
(2) Love, J. C.; Estroff, L. A.; Kriebel, J. K.; Nuzzo, R. G.; Whitesides, G. M. *Chem. Rev.* **2005**, *105*(4), 1103–1169.
(3) Bent, S. F. *Surf. Sci.* **2002**, *500*(1−3), 879–903.
(4) Ashkenasy, G.; Cahen, D.; Cohen, R.; Shanzer, A.; Vilan, A. *Acc. Chem. Res.* **2002**, *35*(2), 121–128.
(5) Lebedev, M. V. *Prog. Surf. Sci.* **2002**, *70*(4−8), 153–186.
(6) Seker, F.; Meeker, K.; Kuech, T. F.; Ellis, A. B. *Chem. Rev.* **2000**, *100*(7), 2505–2536.
(7) Sheen, C. W.; Shi, J. X.; Martensson, J.; Parikh, A. N.; Allara, D. L. *J. Am. Chem. Soc.* **1992**, *114*(4), 1514–1515.
(8) Baum, T.; Ye, S.; Uosaki, K. *Langmuir* **1999**, *15*(25), 8577–8579.
(9) Adlkofer, K.; Tanaka, M. *Langmuir* **2001**, *17*(14), 4267–4273.
(10) Ye, S.; Li, G. F.; Noda, H.; Uosaki, K.; Osawa, M. *Surf. Sci.* **2003**, *529* (1−2), 163–170.
(11) McGuiness, C. L.; Shaporenko, A.; Mars, C. K.; Uppili, S.; Zharnikov, M.; Allara, D. L. *J. Am. Chem. Soc.* **2006**, *128*(15), 5231–5243.
(12) Jun, Y.; Zhu, X. Y.; Hsu, J. W. P. *Langmuir* **2006**, *22*(8), 3627–3632.
(13) Ding, X. M.; Moumanis, K.; Dubowski, J. J.; Tay, L.; Rowell, N. L. *J. Appl. Phys.* **2006**, *99*(5), 054701.
(14) McGuiness, C. L.; Blasini, D.; Masejewski, J. P.; Uppili, S.; Cabarcos, O. M.; Smilgies, D.; Allara, D. L. *ACS Nano* **2007**, *1*(1), 30–49.
(15) McGuiness, C. L.; Shaporenko, A.; Zharnikov, M.; Walker, A. V.; Allara, D. L. *J. Phys. Chem. C* **2007**, *111*(11), 4226–4234.
(16) Wieliczka, D. M.; Ding, X.; Dubowski, J. J. *J. Vac. Sci. Technol., A* **2006**, *24*, 1756–1759.
(17) Yamamoto, H.; Butera, R. A.; Gu, Y.; Waldeck, D. H. *Langmuir* **1999**, *15* (25), 8640–8644.
(18) Schvartzman, M.; Sidorov, V.; Ritter, D.; Paz, Y. *J. Vac. Sci. Technol., B* **2003**, *21*(1), 148–155.
(19) Lim, H.; Carraro, C.; Maboudian, R.; Pruessner, M. W.; Ghodssi, R. *Langmuir* **2004**, *20*(3), 743–747.
(20) Gu, Y.; Lin, Z.; Butera, R. A.; Smentkowski, V. S.; Waldeck, D. H. *Langmuir* **1995**, *11*(6), 1849–1851.
(21) Tanzer, T. A.; Bohn, P. W.; Roshchin, I. V.; Greene, L. H.; Klem, J. F. *Appl. Phys. Lett.* **1999**, *75*(18), 2794–2796.
(22) Stine, R.; Petrovykh, D. Y. *J. Electron Spectrosc. Relat. Phenom.* **2009**, *172* (1), 42–46.
(23) Petrovykh, D. Y.; Yang, M. J.; Whitman, L. J. *Surf. Sci.* **2003**, *523*(3), 231–240.
(24) Ulman, A. *Chem. Rev.* **1996**, *96*(4), 1533–1554.
(25) Buriak, J. M. *Chem. Rev.* **2002**, *102*(5), 1271–1308.

DOI: 10.1021/la804314j

effective for passivating III−V semiconductors *both* chemically and electronically.[6−13,17−19,21]

We investigate the formation of alkanethiol SAMs on InAs(001) surfaces and the potential of SAM-passivated InAs-based field-effect transistors (FETs) as sensors. InAs offers a combination of unique material properties for FET-based sensors.[23,26] In contrast to other III−V semiconductors, the surface Fermi level in InAs is typically pinned *above* the conduction band minimum, which creates a subsurface two-dimensional electron gas (2DEG).[23,26−30] The ultrathin (10−20 nm) InAs films typical in FET and quantum well (QW) devices,[31−34] however, impose a challenging limitation on passivation treatments—+surface etching cannot exceed 1−2 nm.[23,26] For example, an acid etch, which is commonly employed to provide a clean and oxide-free semiconductor surface for SAM formation,[9,13,21] is not sufficiently well controlled for etching ultrathin FETs.

Here we demonstrate how SAMs can be prepared on InAs(001) from an ethanolic solution containing a small amount of aqueous NH_4OH, following the approach used to prepare SAMs on GaAs.[8,11] This "base-activated" method removes the native oxide layer and produces a stable high-density SAM without excessively etching the InAs surface. We compare the characteristics of SAMs on InAs to properties of SAMs on related III−V semiconductors, such as GaAs[7−16] and InP,[17−20] in order to elucidate the element- and material-dependent surface and interface chemistry of SAM formation. Finally, we test the stability of SAMs on InAs against exposure to air and to aqueous solutions, as such stability in ambient environments is critical for sensor applications.

2. Materials and Methods

2.1. Materials. InAs samples of ∼1 cm^2 in size were cut from single-side polished undoped (intrinsically *n*-type) InAs(001) wafers (Princeton Scientific Corporation, Princeton, NJ).[35] We found that extensive degreasing/cleaning of InAs substrates was necessary for producing SAMs consistently: before passivation, samples were soaked in hexanes (HPLC grade) for at least 1 h; sonicated for 5 min successively in hexanes, anhydrous ethanol (Warner-Graham Corp., Cockeysville, MD),[35] and acetone (NF/FCC grade); vigorously rinsed with ethanol; and dried under flowing N_2.

Octadecanethiol $CH_3-(CH_2)_{17}-SH$ (denoted as ODT hereafter) was purchased from Aldrich[35] and purified by recrystallization from ethyl acetate. Passivating solution was prepared by dissolving 143 mg of ODT in 100 mL of ethanol and mixing 9 parts (by volume) of this solution with 1 part aqueous NH_4OH (29.7%, ACS PLUS grade). For deposition experiments conducted under anhydrous conditions, anhydrous 2 M ethanolic NH_3 was purchased from Sigma Aldrich.[35]

2.2. Deposition of SAMs. To prepare SAMs, each InAs sample was placed into 3 mL of ODT solution in a glass vial covered with plastic film. The standard sample treatment took 45−60 min in vials placed on a hot plate having a surface temperature of 55 °C. Following the ODT deposition, samples were vigorously rinsed with ethanol and dried under a stream of N_2. Samples prepared for XPS analysis were additionally sonicated in ethanol for 30 s.

We note that the reaction solution temperatures could not be measured directly without a solution probe; the data in this paper refer to the temperature of the hot plate surface. For an approximate calibration, we have also measured the temperature of water in an open vial placed on the same hot plate. The water temperatures in a vial were 32, 37, and 57 °C at hot plate settings of 50, 60, and 100 °C, respectively. This calibration suggests that the standard deposition of ODT was from solution at ca. 35 °C. Subsequent experiments indicate that an effective deposition can be achieved at higher solution temperatures, in vials that are sealed and placed in a water or oil bath.

For deposition of ODT under anhydrous conditions, two InAs samples were added separately to solutions of ODT (14 mg, 0.05 mmol) in anhydrous 2 M ethanolic NH_3 (5 mL) contained in two thick-walled glass pressure vessels. The vessels were sealed and heated for 12 h at 100 °C in an oil bath and then allowed to reach room temperature. The InAs samples were removed and rinsed successively with ethanol, hexanes, and CH_2Cl_2, and then dried under a stream of N_2.

2.3. Contact Angle and Ellipsometry Measurements. The ODT films deposited under a wide range of conditions were characterized using contact angle (CA) goniometry. The CA of water droplets was measured using a VCA-Optima goniometer (AST Products, Inc., Billerica, MA)[35] within 3−4 s after applying the droplets to the surface.

Spectroscopic ellipsometry data were obtained over a spectral range from 267 to 2091 nm using a variable-angle instrument set sequentially to incident angles of 65°, 70°, and 75°. The manufacturer-supplied software (VASE for Windows, J. A. Woolam Co., Inc., Lincoln, NE)[35] was used to acquire and analyze the variable-angle spectroscopic ellipsometry (VASE) data set. This VASE data set was interpreted assuming a three-layer model that consisted of bulk InAs, an interfacial layer, and an ODT layer. In order to minimize contributions from sample oxidation and contamination, VASE was performed on freshly prepared samples, which were exposed to ambient air for <1.5 h during the VASE measurements and then transferred into an ultrahigh vacuum (UHV) chamber for XPS analysis.

2.4. XPS Characterization of SAMs. X-ray photoelectron spectroscopy (XPS) was performed in a commercial UHV system (1×10^{-9} Torr base pressure) equipped with a monochromatic Al Kα source, a hemispherical electron energy analyzer (58° angle between monochromator and analyzer), and a magnetic lens (nominal analysis spot ≤ 1 mm^2).[36,37] The binding energies (BEs) are reported with 0.1 eV precision, based on a two-point analyzer energy calibration described in detail elsewhere.[36−38] Normal-emission angle-integrated scans were acquired at 0.36 eV analyzer resolution for the As 3d, In 3d, O 1s, C 1s, and S 2p regions, and at 0.9 eV resolution for As 2p. A convolution of Lorentzian and Gaussian line shapes was used to fit the individual peaks; a linear combination of Shirley and polynomial functions was used to model the inelastic electron background, with the corresponding coefficients fit simultaneously with the peaks.[36−39] The electron attenuation length (EAL) values for quantitative

---

(26) Petrovykh, D. Y.; Long, J. P.; Whitman, L. J. *Appl. Phys. Lett.* **2005**, *86*(24), 242105.

(27) Lowe, M. J.; Veal, T. D.; Mowbray, A. P.; McConville, C. F. *Surf. Sci.* **2003**, *544*(2−3), 320–328.

(28) Lowe, M. J.; Veal, T. D.; McConville, C. F.; Bell, G. R.; Tsukamoto, S.; Koguchi, N. *Surf. Sci.* **2003**, *523*(1−2), 179–188.

(29) Olsson, L. O.; Andersson, C. B. M.; Hakansson, M. C.; Kanski, J.; Ilver, L.; Karlsson, U. O. *Phys. Rev. Lett.* **1996**, *76*(19), 3626–3629.

(30) Le Lay, G.; Oughaddou, H. *J. Phys.: Condens. Matter* **2001**, *13*(49), 11195–11206.

(31) He, Z. Q.; Ilver, L.; Kanski, J.; Nilsson, P. O.; Songsiriritthigul, P.; Holmen, G.; Karlsson, U. O. *Appl. Surf. Sci.* **1996**, *104*, 608–614.

(32) Yamaguchi, H.; Sudijono, J. L.; Joyce, B. A.; Jones, T. S.; Gatzke, C.; Stradling, R. A. *Phys. Rev. B* **1998**, *58*(8), R4219–R4222.

(33) Dayeh, S. A.; Soci, C.; Yu, P. K. L.; Yu, E. T.; Wang, D. *J. Vac. Sci. Technol., B* **2007**, *25*(4), 1432–1436.

(34) Cheng, K. A.; Yang, C. H.; Yang, M. J. *J. Appl. Phys.* **2000**, *88*(9), 5272–5276.

(35) Certain vendors and commercial instruments are identified to adequately specify the experimental procedure. In no case does such identification imply endorsement by the Naval Research Laboratory.

(36) Petrovykh, D. Y.; Kimura-Suda, H.; Tarlov, M. J.; Whitman, L. J. *Langmuir* **2004**, *20*(2), 429–440.

(37) Petrovykh, D. Y.; Sullivan, J. M.; Whitman, L. J. *Surf. Interface Anal.* **2005**, *37*(11), 989–997.

(38) Petrovykh, D. Y.; Kimura-Suda, H.; Opdahl, A.; Richter, L. J.; Tarlov, M. J.; Whitman, L. J. *Langmuir* **2006**, *22*(6), 2578–2587.

(39) Hesse, R.; Chasse, T.; Szargan, R. *Fresenius' J. Anal. Chem.* **1999**, *365*(1−3), 48–54.

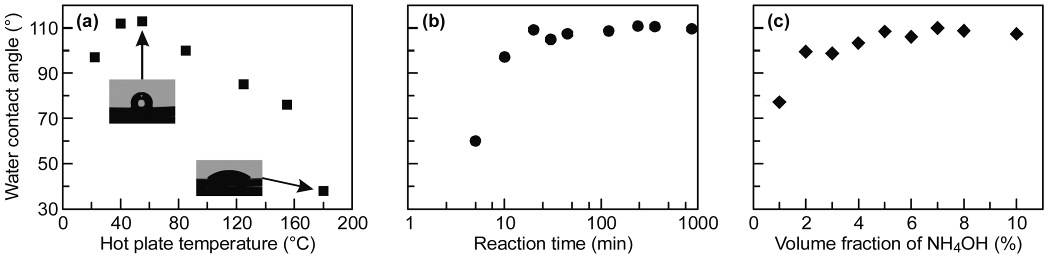

Figure 1. Survey of water CA values for ODT films deposited on InAs under different conditions. For hydrophobic ODT monolayers, the CA values are correlated with surface coverage. The CA dependence on the deposition temperature (a) shows a clear maximum near the hot plate setting of 55 °C, which corresponds to ca. 35 °C solution temperature. The CA values plateau as a function of the reaction time (b) and NH_4OH concentration (c). At NH_4OH volume fraction above 10%, ODT becomes insoluble.

XPS analysis were calculated using NIST SRD-82 software,[40,41] as described in detail previously.[36−38]

2.4.1. Angle-Resolved XPS (*ARXPS*). ARXPS was performed in a commercial UHV system (1×10^{-9} Torr base pressure) equipped with a focused monochromatic Al $K\alpha$ source, a hemispherical electron energy analyzer, a multichannel photoelectron detector, and an automated tilt stage. The instrument control software for this system includes a compucentric tilt procedure, which has been calibrated and tested on each sample prior to ARXPS measurements. Angle-resolved scans were acquired at 0°, 20°, 40°, and 60° emission angles for the As 3d, In 3d, In 4d, O 1s, C 1s, S 2p, and As 2p regions, with instrumental resolution of ca. 0.6 eV. Each of these extended ARXPS data sets was acquired over approximately 1.5 h. In separate testing, we have found that continuous exposure to the X-ray beam for 2 h produces up to 10−15% decrease in the measured ratio of C 1s and As 3d intensities. Accordingly, we also acquired a control ARXPS data set of As 3d, C 1s, and S 2p regions (acquired in $<$ 40 min) to reduce damage to the film during the measurement. Vendor-provided software (Avantage version 4.30, Thermo Fisher Scientific, Inc., East Grinstead, U.K.)[35] was used to calculate overlayer thicknesses based on ARXPS data, assuming both single- and double-layer models.

3. Experimental Results

3.1. Optimization of Deposition Parameters for ODT on InAs. To compare ODT films formed under a wide range of deposition conditions, we used water contact angle (CA) measurements, which proved more practical for exploratory surveys than time-consuming XPS analysis. Water CA values of hydrophobic ODT monolayers are correlated with ODT surface coverages: low-coverage ODT films typically exhibit lower CA values.[10,11,19] We systematically quantified water CA values for ODT films on InAs(001) as a function of three parameters: reaction temperature, time, and concentration of NH_4OH in the passivating solution (Figure 1).

The *reaction temperature* is an important parameter to be considered for SAM deposition and formation. While the archetypal SAMs on Au are usually formed at room temperature over several hours, III−V semiconductor substrates are more chemically active than Au; thus, at room temperature, deposition of ODT must compete against other surface chemical reactions, such as oxidation. For example, Allara and co-workers found that room temperature deposition of ODT on GaAs required rigorously degassing the thiol solution.[11] An alternative approach was suggested by our previous results on chemical passivation of InAs at elevated temperature in basic solutions of thioacetamide, which did not require degassing.[26,37] Accordingly, we explored ODT deposition on InAs from ethanolic thiol solutions made basic by the addition of aqueous NH_4OH and held at elevated temperature (Figure 1a). We achieve the maximum CA value around 55 °C (Figure 1a), indicating that an optimal reaction temperature exists for depositing ODT on InAs. The optimal hot plate setting of 55 °C used in the subsequent experiments corresponds to ca. 35 °C solution temperature. We note that these reaction conditions are similar to those reported by Uosaki and co-workers, who studied the formation of alkanethiolate SAMs on GaAs at elevated temperature using ethanolic thiol solutions containing aqueous NH_4OH.[8]

Scheme 1. Deposition of ODT on InAs(001) from Base-Activated Ethanolic Solution

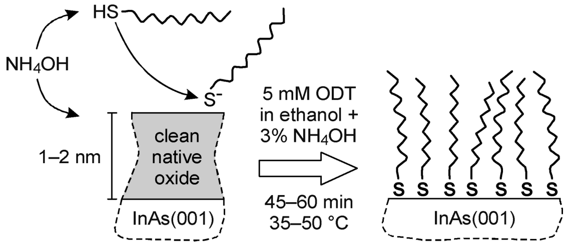

The measured CA values monotonically depend on the duration of the passivation treatment up to ca. 30 min and plateau thereafter (Figure 1b). We have used 45−60 min as the standard length of the ODT deposition for subsequent experiments, in order to consistently produce films that exhibited maximum CA values.

The concentration of aqueous NH_4OH in the deposition solution was previously found to be important for SAM formation on GaAs surfaces.[8] The data in Figure 1c indicate that at NH_4OH volume fraction $\geq 2\%$ our deposition procedure is relatively insensitive to the NH_4OH concentration. At volume fraction $> 10\%$, however, ODT becomes insoluble. The pH values of the deposition solution measured using pH-indicator paper (pHydrion)[35] monotonically increase from 9 for 1% NH_4OH to 10.5 for 10% NH_4OH.

After establishing a set of standard deposition parameters for ODT (Scheme 1), we examined the deposition of alkanethiols with three different lengths of alkane chains. All three depositions produced hydrophobic surfaces; the measured CA values were 89°, 97°, and 110° for chains of 7, 16, and 18 carbon atoms, respectively. A slow increase of the CA values with the chain length is similar to that observed for alkanethiol SAMs on gold and other metals.[1,2,38]

3.2. ODT/InAs(001) Interface Chemistry. The survey and high-resolution elemental XPS data in Figure 2 provide three important spectroscopic signatures of the ODT/InAs(001)

---

(40) Jablonski, A.; Powell, C. J. *Surf. Sci. Rep.* **2002**, *47*(2−3), 35–91.

(41) Powell, C. J.; Jablonski, A. *NIST Electron Effective-Attenuation-Length Database*, version 1.0 (SRD-82); U.S. Department of Commerce, National Institute of Standards and Technology: Gaithersburg, MD, 2001.

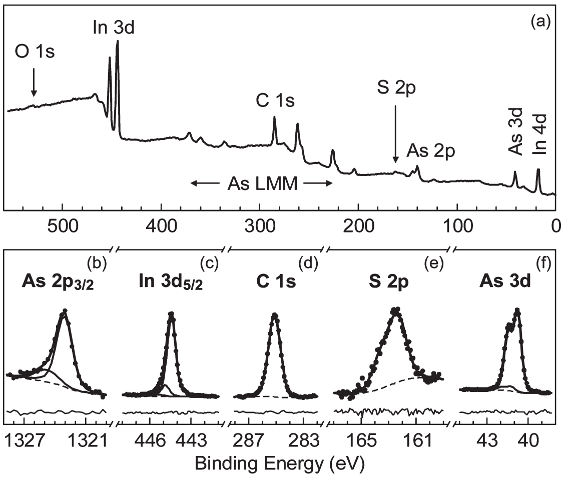

Figure 2. XPS data for an ODT monolayer on InAs immediately after deposition. The survey spectrum (a) indicates minimal oxidation and shows the C 1s and S 2p peaks characteristic of an ODT monolayer. Elemental XPS data (b−f) characterize the ODT/InAs interface chemistry in detail. The submonolayer amount of As−O_X contributes a shoulder in the As 2p region (b) but is not detectable at BE > 44 eV in the As 3d region (f). In the In 3d region (c), an In−S and a barely detectable In−O_X component are present. Symbols = raw data; thin lines = fit components; dashed lines = backgrounds; thick lines = fit sum curves; thin lines at bottom of panels (b−f) = fit residuals.

Table 1. XPS Peak Parameters for ODT/InAs

peak	BE (eV)[a]	spin−orbit intensity ratio	spin−orbit splitting (eV)	FWHM (eV) Lorentz.	FWHM (eV) Gauss.
S 2p	162.3	0.5[b]	1.2[b]	0.15	1.45
C 1s	285.1			0.10	1.00
In 3d					
In−As	444.4	0.67	7.58	0.36	0.49
In−S	444.9[b]	0.67	7.58	0.36	0.49
In−O_X	445.4	0.67	7.58	0.36	0.80
As 3d					
As−In	40.8	0.69[b]	0.69	0.19	0.56
As[c]	41.3	0.69[b]	0.69	0.19	0.56
As $2p_{3/2}$					
As−In	1323.1			0.5[b]	1.5
As−O_X	1324.8			0.5[b]	2.2
As−O[d]	1326.8			0.5[b]	2.3

[a] BE of the higher intensity component for spin−orbit doublets. [b] Fixed parameter value from ref 37. [c] Small "surface component", 6% of the main As 3d intensity. [d] Reference value for native oxide.

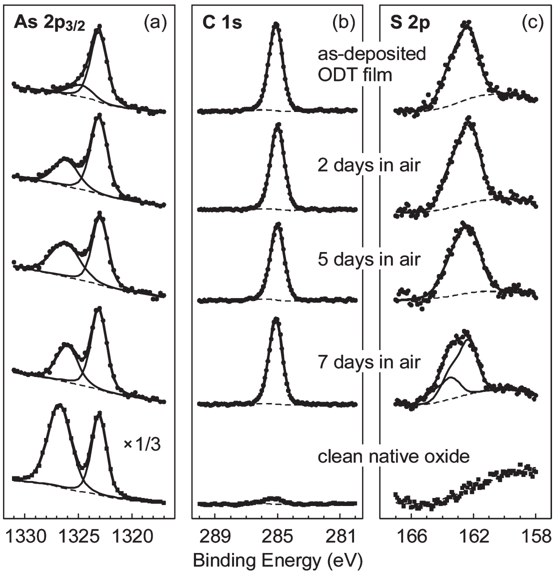

Figure 3. High-resolution XPS data for ODT monolayers on InAs after exposure to air. With increasing exposure to air, the high-BE As−O_X component (a) increases, C 1s (b) and S 2p (c) peaks remain nearly constant. Bottom set of spectra (squares) is for a rigorously degreased InAs(001) wafer with native oxide. Symbols = data; thin lines = fit components; dashed lines = backgrounds; thick lines = fit sum curves. For comparison between samples, data are normalized to the intensity of the bulk As 3d component for each sample.

interface chemistry. First, an In−S component can be clearly identified in the In 3d region (Figure 2c), whereas As−S components are not observed in the As 2p and 3d regions (Figure 2b and 2f). Second, the S 2p doublet parameters (Figure 2e and Table 1) are similar to those reported for S-passivated InAs(001).[23,26,37,42,43] Third, a barely detectable In−O_X component (Figure 2c) and minimal intensities of O 1s peak (Figure 2a) and As−O_X component (Figure 2b) indicate that the native oxide layer is removed during the base-activated ODT deposition (Scheme 1), and thus, the sulfur bonding occurs on essentially a clean In-terminated InAs(001) surface. Notably, there is no detectable As−O_X component around ca. 44 eV in the As 3d region (Figure 2f), so a freshly prepared ODT/InAs surface is essentially "oxide-free" in terms of this conventional metric.[11,37] Instead of the bulk-dominated As 3d region, the As−O_X component in the surface-sensitive As 2p region (Figure 2b) has to be used to detect and quantify the initial oxidation of these surfaces.[37]

The parameters of the S 2p doublet (Table 1) are consistent with ODT molecules that are chemisorbed on InAs via a thiolate bond.[22] The width of the single S 2p doublet in Figure 2e indicates a distribution of S chemical states, comparable to that on S-passivated InAs(001).[23,26,37,42,43] The S 2p BE = 162.3 eV is higher than BE = 161.6 eV observed for S-passivated InAs(001),[37] but the difference between the two values is likely due to the difference between the respective chemical environments. An almost identical S 2p BE difference between thiolate S in ODT and chemisorbed S is observed between ODT/InP (BE = 162.4 eV) and S/InP (BE = 161.6 eV).[19]

3.3. Stability of the ODT/InAs Interface against Oxidation in Air. We used XPS to track oxidation of the ODT/InAs interface (Figure 3), thus obtaining a quantitative measure of the effectiveness of the chemical passivation provided by ODT monolayers.[23,26,37,38] The As 2p region (Figure 3a) furnishes a particularly sensitive measurement of the surface oxide, because the corresponding EAL is < 1 nm.[26,37]

The high-BE As 2p component for the as-deposited ODT/InAs sample exhibits a BE chemical shift of < 2 eV from the bulk As−In component (Figure 3a, Table 1). The chemical shift reported for As^{3+} oxide is at least 3 eV;[44] therefore, a smaller shift indicates limited surface oxidation. An alternative assignment for this high-BE As 2p component is As−S, because a BE shift of 1.65 eV has been reported for As−S on GaAs(100) sulfidized in an

---

(42) Fukuda, Y.; Suzuki, Y.; Sanada, N.; Shimomura, M.; Masuda, S. *Phys. Rev. B* **1997**, *56*(3), 1084–1086.
(43) Ichikawa, S.; Sanada, N.; Utsumi, N.; Fukuda, Y. *J. Appl. Phys.* **1998**, *84* (7), 3658–3663.
(44) Hollinger, G.; Skheytakabbani, R.; Gendry, M. *Phys. Rev. B* **1994**, *49*(16), 11159–11167.

aqueous $(NH_4)_2S$ solution.[45] This assignment ambiguity has been previously discussed for an As 2p component with similar BE and intensity on InAs treated with thioacetamide.[37]

The extended exposure to ambient air results in oxidation of the ODT/InAs interface, as evidenced by the increasing high-BE As 2p components in Figure 3a (top-to-bottom). Both the degree of oxidation and the amount of As oxides after ODT-passivation are comparable to or lower than those after S-passivation.[23,26,37] After 2−7 days of air exposure, the high-BE As 2p component remains at ca. 3.0 eV above the bulk As−In peak; that is, the interface does not reach the oxidation level of a native oxide film, where the As−O_X peak appears ca. 4.0 eV above the bulk peak (Table 1, bottom of Figure 3a). The amount of As−O_X detected in the surface-sensitive As 2p region after 1 week in air is ca. 30% of the native oxide level. The stability of ODT/InAs against reoxidation is, therefore, comparable to that of ODT/GaAs, where ca. 20% of the native oxide level is reported after 2 weeks in air, based on the less surface-sensitive As 3d.[11]

The intensity of C 1s and S 2p peaks remains constant under exposure to ambient air (Figure 3b and 3c), indicating that ODT monolayers on InAs are stable against the loss of constituent molecules even as the ODT/InAs interface slowly oxidizes. After 7 days, a high-BE S 2p component emerges, most likely due to the increased ODT/InAs interface oxidation. Comparison of the S 2p spectra acquired for ODT/InAs and for the native oxide control sample (Figure 3c) also clearly shows that, in contrast to ODT/GaAs, where an overlapping Ga substrate peak complicates fitting of the S 2p spectrum,[11,12] on InAs the background signal has a smooth and stable shape that is readily modeled when fitting the S 2p doublet.[37]

3.4. Stability of ODT/InAs in Solutions. To test the stability of ODT/InAs in liquid environments, we exposed samples to organic solvents and aqueous solutions. For a stringent test of stability against organic solvents, we soaked ODT-treated InAs chips for extended periods in CH_2Cl_2, in which ODT is more soluble than in ethanol. After 17 h in CH_2Cl_2, the CA values for ODT films decreased by ca. 10−20°. The higher stability against the CH_2Cl_2 exposure (smaller decrease of CA) was generally correlated with higher as-deposited hydrophobicity, that is, higher CA values in Figure 1. All ODT films on InAs remained hydrophobic after the CH_2Cl_2 soak, but apparently were less stable against the CH_2Cl_2 exposure than ODT SAMs formed on coinage metals.[2,38]

Stability in aqueous solutions is a critical property for many practical applications of semiconductor surfaces protected by SAMs. We have exposed ODT monolayers on InAs to two types of aqueous environments: deionized water and a standard phosphate-buffered saline (PBS) buffer. After a soak in *deionized* water for 17 h, the water CA drops to 32°, essentially the same value as that observed for a clean InAs native oxide surface. This apparent removal of ODT films from InAs in deionized water is in contrast to the behavior of hydrophobic SAMs on coinage metals,[2] but it is similar to the observations for ODT SAMs on GaAs.[14]

The ODT monolayers on InAs are considerably more stable in PBS buffer (0.14 M NaCl, 3 mM KCl, pH 7.4) than in deionized water. After immersion for 1 h in PBS buffer, the water CA decreases by only 6°, remaining above 100°. After 7 h in PBS buffer, the water CA value drops by 15° but still remains above 90°, so the surface remains hydrophobic. The stability of ODT/InAs in PBS buffer was confirmed by electrochemical measurements (Figure 4). An area ca. 0.5 cm^2 was masked off on the InAs samples using nail polish and contacted with leads In-soldered to the surface. A continuous ODT monolayer deposited on such a *conductive* InAs surface (used as the working electrode) is expected to suppress the non-Faradic current during a cyclic voltammetry (CV) experiment. After the ODT deposition, the current is suppressed by at least a factor of 10 (black curve in Figure 4) compared to the control measurement on a clean InAs native oxide (gray curve in Figure 4).

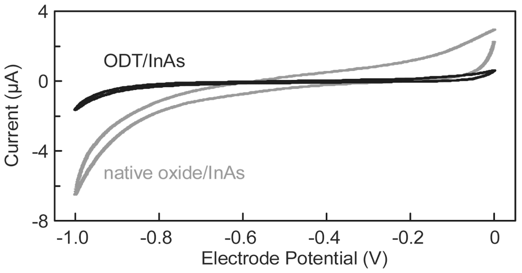

Figure 4. Cyclic voltammograms for InAs surfaces in PBS buffer. The CV data are shown for a clean InAs native oxide (gray) and for InAs after the deposition of an ODT monolayer (black), both in PBS buffer (0.14 M NaCl, 3 mM KCl, pH 7.4). The current flow is suppressed after the ODT deposition.

4. Analysis and Discussion

4.1. Formation of ODT Monolayers on InAs(001). Facile deposition, attachment, and diffusion of alkanethiols on coinage metals gives rise to many special properties of the resulting SAMs.[1,2] Because of the dramatically different behavior of alkanethiols on III−V semiconductors, we should not assume *a priori* that the resulting monolayers have properties similar to those of SAMs on metals. In a recent comprehensive examination of alkanethiol monolayers prepared on GaAs, the observation of both molecular ordering and reversibility of the attachment chemistry confirmed that these monolayers are true SAMs.[11,14,15] Because the standard deposition conditions for our version of the base-activated method (Scheme 1) are different from those used for preparing SAMs on GaAs, we now consider how the formation of SAMs can be affected by deposition time, temperature, and the presence of oxygen.

Previous results for SAM deposition on two III−V materials related to InAs− GaAs and InP− provide conflicting evidence for the effect of oxygen during deposition. Allara and co-workers reported that rigorous deoxygenation of the deposition solutions was crucial for preparing SAMs on GaAs,[11] presumably because, in the presence of oxygen, an oxide layer formed before the majority of thiolated molecules could attach to the surface. The observation of oxidation of GaAs in several other studies indirectly supports the importance of oxygen-free handling.[12,16,46] In contrast, ODT monolayers have been prepared on InP (after HF-stripping the native oxide) under ambient conditions and without base-activation.[19] Our observation of minimal oxidation of InAs for as-deposited samples (Figure 2) indicates that oxygen-free handling is less critical for preparing SAMs on InAs (when base-activation is used) than on GaAs.

The relatively short deposition time used in our work (45−60 min versus day-long depositions in previous studies[11,19]) may have helped to minimize the surface oxidation and to avoid another potential problem. Oxygenated basic solutions induce formation of disulfide-bonded thiol dimers, and such dimers do not readily react with III−V semiconductors.[11] The thiol

---

(45) Lebedev, M. V.; Mayer, T.; Jaegermann, W. *Semiconductors* **2004**, *38*(2), 153–160.

(46) Mohaddes-Ardabili, L.; Martinez-Miranda, L. J.; Silverman, J.; Christou, A.; Salamanca-Riba, L. G.; Al-Sheikhly, M. *Appl. Phys. Lett.* **2003**, *83*, 192–194.

dimerization reaction is efficient but slow, requiring hours or days to complete; the disulfide formation in our basic deposition solutions apparently was not significant over the typical deposition times.

The apparent ODT film formation kinetics (Figure 1b) are faster in our version of the base-activated deposition than the kinetics reported for deposition of ODT on GaAs.[11] Accordingly, the ODT monolayers on InAs are likely formed in a kinetically driven rather than a quasi-equilibrium (and reversible) process; therefore, these monolayers may not satisfy the strict definition of SAMs.[11] We agree with Allara and co-workers that a quasi-equilibrium and reversible deposition process is likely to be critical to produce ordered SAMs of ODT on GaAs;[11] the different conditions used in our work are likely to produce films with lower degree of ordering than that observed for ODT/GaAs. Our ability to deposit ODT monolayers on InAs at temperatures as high as 100 °C (described below) does, however, suggest that a wide range of kinetic parameters is acceptable for forming ODT films using our approach.

The deposition temperature dependence in Figure 1a is surprising, because moderately increasing the solution temperature should increase the diffusion rates and thus improve the ability of ODT molecules to fill surface binding sites, which is likely to be the limiting factor in forming dense monolayers. The decreasing CA values for films deposited at hot plate temperatures > 55 °C (Figure 1a) are likely due to selective evaporation of NH_3 at elevated solution temperatures. The reaction vials were sealed with flexible plastic film, but such seals might be partially permeable for a molecule as small as NH_3. Moreover, the equilibrium partition of NH_3 between the gas and solution phases will shift toward the gas phase at elevated solution temperatures. To test this explanation, we carried out the ODT deposition in anhydrous 2 M ethanolic NH_3 at 100 °C in sealed pressure vessels. The resulting CA values of the ODT films were comparable to those obtained under our optimized conditions (CA $\geq 100°$), indicating that NH_3 evaporation likely dominates the temperature dependence of CA values in Figure 1a.

Changes in solution temperature also likely affect the etch rates and solubilities of different species created in surface reactions. We note, however, that the overall etch rate of InAs(001) previously observed under similar solution conditions had been significantly smaller than 1 nm/min,[23,26] so the principal effect of the solution temperature is likely to be a change in relative solubilities of the different surface species (e.g., oxides versus sulfides), rather than significant changes of the surface etch rate.

4.2. Structure of the ODT/InAs(001) Interface. A "layer-cake" structure has been previously proposed for S-passivated InAs(001): S chemisorbed on top of an In-terminated InAs(001) surface.[23,26,37] In other words, the characteristic XPS signature of S-passivated InAs(001) includes In−S but not As−S bonds.[23,26,37] In contrast, on the prototypical S-passivated GaAs(001), both Ga−S and As−S bonds (and elemental As) have been observed.[5,47,48] In Figure 2, there are In−S but not As−S components, which together with the S 2p peak parameters (Table 1) and minimal InAs oxidation (Figure 2) are consistent with a layer-cake-like structure of the ODT/InAs(001) interface: ODT molecules chemisorbed on In-terminated InAs(001) via thiolate bonds. The spectral signatures of the In−S bonding and the absence of S-bonding features for the respective V elements are common properties of sulfur-based chemistry (inorganic and organic) on InAs(001) and InP(001).[17,19,23,26,37] In contrast, exclusive As−S or mixed Ga−S/As-S bonding is reported for thiols on GaAs(001).[10−12,14,15] Finally, we note that the apparent dependence of the surface chemistry of III−V materials on the individual elements *and* the respective compounds is consistent with results of a recent systematic study of III−V surface passivation by pH-activated organic sulfide (thioacetamide).[49]

4.3. Structure of ODT Films on InAs(001). Three important characteristics of ODT films produced on InAs(001) by the base-activated method (Scheme 1) can be determined from quantitative analysis of data obtained by XPS and ARXPS, which are recognized as reliable techniques for characterizing surface density, thickness, and interface chemistry for SAMs.[1,12,19,22,36,38,50−53] We begin by ruling out multilayer formation, which, in principle, is possible when ODT is deposited from a poor solvent, such as ethanol. We then proceed to estimate the surface coverage of ODT molecules in these films to be approximately 1 monolayer (ML). Finally, we find that the ARXPS profiles and C/S stoichiometry measured for these monolayers are consistent with an upright average orientation of ODT chains.

4.3.1. S 2p Chemical Signature. The first indication that the base-activated deposition produces at most a *monolayer* rather than multilayers of ODT on InAs comes from the BE of the S 2p doublet (Figure 2e, Table 1). The absence of S 2p intensity at 163−165 eV BE indicates that any multilayers or otherwise weakly bound ODT molecules represent a negligibly small fraction of these ODT films.[12,53]

4.3.2. Angle-Resolved XPS Analysis. We used ARXPS to measure nondestructively the thickness and elemental profile of ODT films on InAs. The software developed by the instrument manufacturer includes automated routines for several types of ARXPS data analysis, and results from two of the routines are presented in Figure 5.

The relative-depth analysis routine provides a model-independent interpretation of ARXPS data, by calculating the relative average depth of the elements based only on the respective measured angle-dependent intensity ratios. This type of analysis is particularly effective for identifying stratification of specific "signature" elements in layered systems, such as that shown in the diagram for ODT/InAs (Figure 5a). This qualitative depth profile indicates that both In and As are located within the lowest layer (labeled as "substrate"), S and O are within an "interface" layer above the substrate, and C is within the topmost layer (labeled as "film"). We note that the underlying algorithm is sufficiently robust to have identified both As 3d and 2p signals as coming from the substrate, even though the respective photoelectrons have dramatically different sampling depths, because of > 1000 eV difference in their BE.[37] This coassignment of the two As peaks confirms that the algorithm is primarily sensitive to the angle-dependence of intensity ratios, rather than the physical depth from which the photoelectrons originate.

The qualitative depth profile from Figure 5a is useful for identifying an appropriate structure model, which is required

---

(47) Xu, F. Q.; Lu, E. D.; Pan, H. B.; Xie, C. K.; Xu, P. S.; Zhang, X. Y. *Surf. Rev. Lett.* **2001**, *8*(1−2), 19–23.

(48) Bessolov, V. N.; Zhilyaev, Y. V.; Konenkova, E. V.; Lebedev, M. V. *Tech. Phys.* **1998**, *43*(8), 983–985.

(49) Stine, R.; Aifer, E. H.; Whitman, L. J.; Petrovykh, D. Y. *Appl. Surf. Sci.* **2009**, *255*(16), 7121–7125.

(50) Folkers, J. P.; Laibinis, P. E.; Whitesides, G. M. *Langmuir* **1992**, *8*(5), 1330–1341.

(51) Laibinis, P. E.; Bain, C. D.; Whitesides, G. M. *J. Phys. Chem.* **1991**, *95*(18), 7017–7021.

(52) van der Marel, C.; Yidirim, M.; Stapert, H. R. *J. Vac. Sci. Technol., A* **2005**, *23*(5), 1456–1470.

(53) Castner, D. G.; Hinds, K.; Grainger, D. W. *Langmuir* **1996**, *12*(21), 5083–5086.

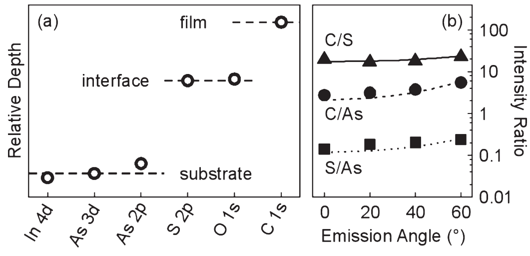

Figure 5. Analysis of ARXPS data for ODT monolayer on InAs. A qualitative analysis of angle-dependent intensity ratios indicates the distribution of elements (a) stratified into three layers: In and As in the substrate, S and O at the ODT/InAs interface, and C in the topmost film. A corresponding quantitative model (b) is used to determine thicknesses of the C-containing film and S-containing interfacial layer from simultaneous fits (lines) of the experimental angle-dependent intensity ratios (symbols) between C 1s, S 2p, and As 3d peaks.

for quantitative ARXPS analysis. The elemental distribution in Figure 5a clearly suggests a model that includes a substrate and two overlayers. The ARXPS analysis algorithm implemented in the instrument software assumes an exponential attenuation of photoelectrons in each of the three layers with EALs calculated for each layer using the TPP-2M formula.[54,55] The best simultaneous fits of C 1s, S 2p, and As 3d pairwise intensity ratios shown in Figure 5b correspond to the carbon layer thickness of 1.8 ± 0.2 nm and S-based interface layer thickness of 0.30 ± 0.05 nm. These results are in agreement with single-layer calculations that estimate the total thickness of the ODT layer as 2.2 ± 0.2 nm and the sulfur layer thickness as 0.30 ± 0.05 nm.

4.3.3. Estimating Film Thickness from Normal-Emission XPS Data. Having the results of ARXPS analysis allows us to evaluate a more general method for estimating thicknesses of overlayers in situations where only basic XPS data (e.g., "atomic %") are available. The standard XPS formalism provides the following expression for a Scofield-normalized XPS intensity ratio for a carbonaceous overlayer (C) on a substrate (X):[36-38,40]

$$\frac{I_{\mathrm{C}}}{I_{\mathrm{X}}}\frac{\sigma_{\mathrm{X}}}{\sigma_{\mathrm{C}}} = \frac{T_{\mathrm{C}}}{T_{\mathrm{X}}}\frac{L_{\mathrm{C}}^{\mathrm{Q}}}{L_{\mathrm{X}}^{\mathrm{Q}}}\frac{N_{\mathrm{C}}}{N_{\mathrm{X}}}\frac{1-\exp\left(-\frac{t}{L_{\mathrm{C}}^{\mathrm{SAM}}}\right)}{\exp\left(-\frac{t}{L_{\mathrm{X}}^{\mathrm{SAM}}}\right)} \qquad (1)$$

The parameters in eq 1 are as follows: T, the analyzer transmission function; σ, the total photoelectric cross section (Scofield);[56] N, the elemental atomic density; and t, the overlayer thickness. The two types of EALs are L^{Q} [EAL for quantitative analysis (QEAL)] and L^{SAM} [average practical EALs (PEAL)];[36,40] EAL values have been calculated previously for InAs[37] and alkanethiol SAMs;[38,51] for a thin organic layer, $L_{\mathrm{C}}^{\mathrm{Q}} \approx L_{\mathrm{C}}^{\mathrm{SAM}}$. For detectors set to constant pass energy, T depends on the kinetic energy (KE) of photoelectrons approximately as $T(\mathrm{KE}) \sim \mathrm{KE}^{-0.5}$.[57]

The $I_{\mathrm{C1s}}/I_{\mathrm{As3d}}$ and $I_{\mathrm{C1s}}/I_{\mathrm{In3d}}$ Scofield-normalized normal-emission intensity ratios calculated from eq 1 for C layer thicknesses up to 4 nm are shown in Figure 6. The experimental ratios for ODT (circles in Figure 6) are $(I_{\mathrm{C1s}}/I_{\mathrm{As3d}})^* = 3.26$ and $(I_{\mathrm{C1s}}/I_{\mathrm{In3d}})^* = 3.12$ (* indicates Scofield[56] normalization). The corresponding range of ODT film thicknesses is 1.8−2.2 nm, in good agreement with ARXPS results.

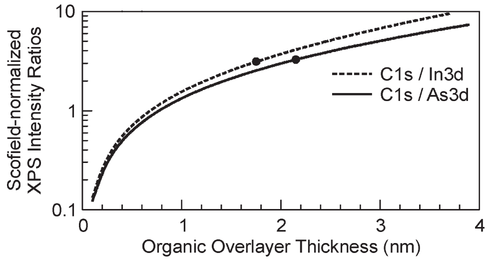

Figure 6. Intensity ratios calculated for major XPS peaks of an organic overlayer on InAs. The ratios are normalized by the corresponding Scofield[56] coefficients (eq 1), in order to simplify the interpretation and comparison with similar data in the "atomic percent" representation. Circles indicate the experimental values of intensity ratios for ODT/InAs(001).

4.3.4. Ellipsometry Measurements. As noted in the previous study of ODT SAMs on GaAs,[11] the presence of a complex interface layer makes interpretation of ellipsometry data for SAMs on III−V semiconductors more difficult than that for SAMs on gold. For fitting the VASE data, we used a three-layer model consisting of bulk InAs, an interfacial layer, and an ODT layer. Optical properties of the interfacial layer were determined from a separate measurement of an InAs sample that had been passivated in a basic thioacetamide solution. This sulfur-passivated sample was chosen as an empirical model of the substrate below the ODT layer because bare InAs samples readily oxidize under ambient conditions, whereas sulfur-passivated InAs surfaces undergo only minimal oxidation in air and are structurally and chemically similar to the interface between ODT and InAs.[26,37,49] The thickness of the ODT layer was determined from a fit of VASE data from the ODT-functionalized sample to a Cauchy layer model with an index of refraction fixed at 1.45.[50]

The thickness of ODT film calculated from VASE data was 24.7 Å, in agreement with the upper limit of values obtained from ARXPS measurements. This optical thickness is also slightly larger than the value of 21 ± 2 Å reported for an ODT monolayer on GaAs.[11]

4.3.5. Is ODT Film a Monolayer or Multiple Layers? Both XPS and ellipsometry measurements indicate that the thickness of ODT films deposited from base-activated solutions is comparable to the nominal length of ODT molecules (2.4 nm). The only multilayer option for producing a film of such thickness is having layers of ODT molecules with chains oriented parallel to the surface. Such a putative multilayer, however, would contain a significant fraction of ODT molecules not directly bound to the substrate, which is contrary to the observed S 2p chemical signatures (section 4.3.1) and to the stability of these films against soaking in $\mathrm{CH_2Cl_2}$. Accordingly, we can rule out multilayer formation under deposition conditions described in Scheme 1.

4.3.6. ODT Surface Coverage. Having established that base-activated deposition produces at most 1 monolayer of ODT on InAs, we can estimate the corresponding ODT surface coverage, based on ratios of S 2p intensity to those of the substrate As 3d and In 3d peaks. The analysis method previously developed for S-passivated InAs[37] is applicable to ODT/InAs. The ODT monolayer, however, is thicker than overlayers on S-passivated InAs, so the measured intensity ratios normalized to the two substrate elements will be affected by the ca. 400 eV difference in KE between As 3d and In 3d photoelectrons, increasing the systematic uncertainty of the coverage estimate. The respective intensity ratios for ODT films are $I_{\mathrm{S2p}}/I_{\mathrm{As3d}} = 0.12$ and $I_{\mathrm{S2p}}/I_{\mathrm{In3d5/2}} = 0.016$, which gives a coverage estimate of 0.8−1.1 ML (using the value 1 ML = 5.4 × 10^{14} atoms/cm^2 previously

---

[54] Tanuma, S.; Powell, C. J.; Penn, D. R. *Surf. Interface Anal.* **1994**, *21*(3), 165–176.

[55] Tanuma, S.; Powell, C. J.; Penn, D. R. *Surf. Interface Anal.* **2005**, *37*(1), 1–14.

[56] Scofield, J. H. *J. Electron Spectrosc. Relat. Phenom.* **1976**, *8*(2), 129–137.

[57] Powell, C. J.; Seah, M. P. *J. Vac. Sci. Technol., A* **1990**, *8*(2), 735–763.

validated for XPS analysis of monolayers on InAs),[37] that is, about half the S coverage on S-passivated InAs and consistent with approximately a full monolayer of ODT. The surface density of ODT on InAs(001) measured by XPS is thus comparable to surface densities of ODT SAMs on metals.[1,2,38,58,59]

4.3.7. Orientation of ODT Molecules. We find strong indications that, in ODT monolayers prepared following Scheme 1, ODT molecules are oriented with organic chains pointing away from the surface. Our ARXPS analysis reveals that the majority of S atoms are located below the C film (Figure 5). The S 2p BE, exclusively corresponding to a thiolate bond at the interface, together with the ARXPS elemental profile indicate that ODT molecules in these monolayers are bound to InAs via thiol groups and that organic chains are oriented away from the surface. All the thickness measurements produced values comparable to the nominal length of ODT molecules—a result consistent with a monolayer of approximately upright ODT molecules. Finally, the measured Scofield-normalized intensity ratio $(I_{C1s}/I_{S2p})^* = 24.7$ is consistent with the theoretical value of 24.8 for a fully upright ODT monolayer.[38] The clean native oxide control in Figure 3b provides an estimate of adventitious carbon contamination for freshly prepared samples in our study. The corresponding C 1s intensity is ca. 8% of that for the ODT film, which corresponds to an uncertainty of thickness and stoichiometry estimates equivalent to one C atom per ODT molecule. While none of these results provide direct measurements of molecular bond orientations, the only film structure consistent with all our observations is a nearly full monolayer of thiol-down ODT molecules with upright average orientation of alkane chains.[60]

4.4. Chemical Stability of ODT/InAs. Chemical passivation against oxidation in air provided by ODT monolayers on InAs(001) is comparable to or better than the passivation produced by inorganic and organic sulfide treatments.[23,26,37] Immediately after the ODT deposition, the amount of $As-O_X$ at the ODT/InAs interface can be estimated from the intensity of the high-BE As 2p component (Figure 3a). Based on the previous calibration,[37] the initial amount of $As-O_X$ is 0.3−0.5 ML (depending on the fraction of that As 2p component assumed to be As−S). Such a small amount of surface oxide on as-deposited samples indicates that base-activated ODT deposition is remarkably effective in removing the native surface oxide, comparable in effectiveness to treatment by basic solutions of thioacetamide.[26,37]

Both the intensity and BE chemical shift of the high-BE As 2p component increase with exposure to air (Figure 3a), but even after 7 days in air the total amount of As oxides remains below 1 ML. The BE chemical shift also remains below that of the native oxide, which suggests that As^{3+} rather than As^{5+} species dominate at the reoxidized ODT/InAs interface. The long-term stability of ODT/InAs against reoxidation in air is thus comparable to the stability of S-passivated InAs surfaces.[26,37]

Extended immersion in an aggressive organic solvent, such as CH_2Cl_2, provides an empirical test of the stability of the ODT/InAs attachment chemistry. For ODT monolayers deposited under the standard conditions (Scheme 1), the water CA decreased after a 17 h soak in CH_2Cl_2, but the surfaces remained hydrophobic (CA values > 90°), indicating that any loss of ODT molecules from these monolayers was not significant. In contrast, for ODT monolayers deposited on InAs under suboptimal conditions, for example, for < 45 min, at hot plate temperatures < 50 °C or > 100 °C (Figure 1), the water CA dropped into the hydrophilic 30−70° range, indicating significant losses of ODT and, accordingly, an unstable interface chemistry. As noted in section 4.1, we believe that the poor quality of films produced at high temperatures (Figure 1a) was related to the loss of NH_3 from the deposition solution.

4.5. Thermal Stability of ODT/InAs. A successful deposition carried out in a sealed vessel at 100 °C in anhydrous ethanolic NH_3 indicates that the ODT/InAs attachment chemistry is stable at least up to that temperature. This thermal stability of ODT/InAs(001) is comparable to the reported stability of ODT/GaAs-(001) up to 80 °C in nitrogen atmosphere.[11] For another related III−V-based system, ODT/InP(001), the surface is reported to remain hydrophobic for up to 100 °C in vacuum but becomes hydrophilic after 30 min immersion in boiling chloroform or water.[19] These results for ODT/InP suggest that the stability of the ODT/InAs surface at 100 °C observed in our experiments may be due in part to the absence of water in the reaction mixture.

4.6. Compatibility with Biosensing Applications. We are exploring InAs as a prospective material for producing biosensors based on field-effect transistors (FETs).[6,23,26] In contrast to other III−V semiconductors, the surface Fermi level of InAs is typically pinned *above* the conduction band minimum, which results in downward band bending at interfaces and formation of a subsurface charge accumulation region.[23,26−30] This high charge density near the surface makes InAs intrinsically conductive even for films and wires having thicknesses < 10 nm.[31−34] In addition, a two-dimensional (2D) electron gas forms at InAs interfaces, causing the surface band bending (and surface conductivity) to be very sensitive to the presence of adsorbates.[23,26,29,30] These unique properties make InAs an attractive candidate for making FET-type biosensors (bioFETs), in which biomolecular binding would be detected by monitoring changes in surface conductance or capacitance.[6,23,26]

The ideal surface treatment for such InAs-based bioFETs should remove the native oxide with minimal etching of the InAs substrate, protect the surface against reoxidation in air and aqueous buffers, preserve the electronic properties of InAs, be thin enough to allow efficient charge sensing, and provide a possible chemical pathway for the attachment of DNA or other biomolecular capture probes.[6,23,26] Deposition of a continuous monolayer of thiolated organic molecules is clearly a promising candidate for a surface treatment that possesses all of the above properties. Accordingly, we have used the base-activated deposition of ODT (Scheme 1) on model InAs devices to test the compatibility of such organic monolayers with the requirements of biosensing applications.

First, we treated InAs/AlSb QW structures with ODT solution, in order to determine the electronic transport properties of prototypical thin (< 100 nm) surface layers of InAs after the ODT deposition. Two QW structures grown on InAs substrates were tested: a "surface-QW" with a 15 nm InAs QW layer exposed at the surface, and a "buried-QW" with an additional InAs QW layer that was electronically coupled to the surface but "buried" under the 15 nm surface InAs layer and an AlSb barrier layer. Hall-effect measurements were used to determine the carrier concentration and mobility in these devices before and after the base-activated ODT surface treatment (Figure 7).

The transport properties of both surface- and buried-QW structures were preserved after the base-activated ODT treatment, as can be clearly seen by comparing the "native" and

---

(58) Kawasaki, M.; Sato, T.; Tanaka, T.; Takao, K. *Langmuir* **2000**, *16*(4), 1719–1728.

(59) Schlenoff, J. B.; Li, M.; Ly, H. *J. Am. Chem. Soc.* **1995**, *117*(50), 12528–12536.

(60) IR spectroscopy is commonly used to measure the chain orientation in SAMs directly. InAs, however, is a narrow-band semiconductor with very strong IR absorbance, which makes IR spectroscopy of molecular monolayers on InAs extremely challenging, whether in reflection or in transmission.

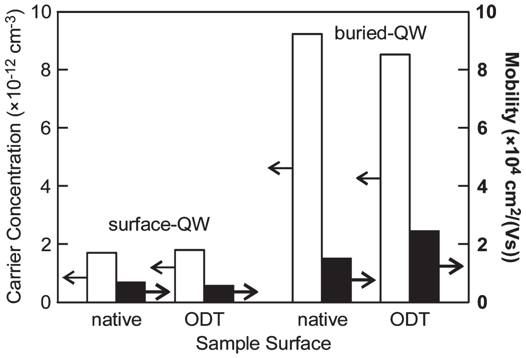

Figure 7. Electronic properties of InAs/AlSb QW structures before and after the base-activated ODT treatment. Carrier concentration (open bars, left axis) and mobility (black bars, right axis) were determined from Hall-effect measurements on QW structures before (native) and after (ODT) the ODT treatment. "surface-QW" and "buried-QW" indicate structures in which transport was dominated by an InAs QW layer, respectively, exposed and not exposed at the device surface.

"ODT" data for each device in Figure 7. Carrier concentration and mobility are sensitive to material defects; therefore, we can conclude that the ODT treatment did not produce excessive or nonuniform etching of these devices. Remarkably, even the exposed ultrathin (15 nm) InAs layer of the surface-QW structure was not significantly damaged by the ODT treatment. The electronic properties of the buried-QW device are dominated by the second "buried" InAs QW layer, which was not exposed to the ambient environment or the solution, which likely explains the higher mobility and carrier concentration values measured for this device both before and after the ODT treatment (Figure 7).

Testing the stability of ODT-passivated devices in an aqueous buffer was the next important step in determining the viability of this treatment for bioFET surfaces. As described in section 3.4, ODT monolayers on InAs(001) are actually unstable in deionized water—a surprising property that they share with ODT SAMs on GaAs(001).[14] Fortunately, the stability of ODT monolayers on III−V semiconductors immersed in aqueous solutions appears to depend on the specific solution properties, for example, ODT monolayers on InP(001) are stable in water at acidic pH but unstable at basic pH.[19] Similarly, as described in section 3.4, the ODT monolayers on InAs(001), while unstable in deionized water, are stable in PBS buffer (pH 7.4), both under a static exposure and in an active electrochemical cell (Figure 4), which represents an environment similar to that of a biosensing device. The stability of the model ODT/InAs surfaces in PBS buffer suggested to us that InAs surfaces of InAs/AlSb QW devices might be similarly protected by the base-activated ODT treatment.

Two InAs/AlSb surface-QW devices were treated in base-activated ODT solution. One device was set aside to serve as a dry control. The other ODT-treated QW device was fitted with a polycarbonate microfluidics chamber and connected to a peristaltic pump. Aqueous buffers with pH 6.8 and 7.7 were prepared from a 200 mM solution of KH_2PO_4 (pH-adjusted by adding HCl). These two pH buffers were alternately pumped through the microfluidics chamber at 80 mL/min. The results of the continuous flow pH-sensing by the surface-QW device are shown in Figure 8.

There is a clear systematic sensor response to alternating pH between 6.8 and 7.7 in Figure 8, once the 40 s transit time delay is taken into account. The current response increases at lower pH and decreases at higher pH. While the data are noisy, these measurements were carried out on an unoptimized device and meant as a simple proof-of-principle test of the surface stability. Clearly, the ODT-passivated InAs/AlSb surface-QW device is capable of performing current measurements under continuous flow of a realistic aqueous buffer solution. The device was left under the flow for ca. 55 min. After the experiment, both the test device and the dry control were stored under dry N_2 atmosphere for ca. 24 h and then analyzed by XPS (Figure 9), in order to check for signs of surface degradation.

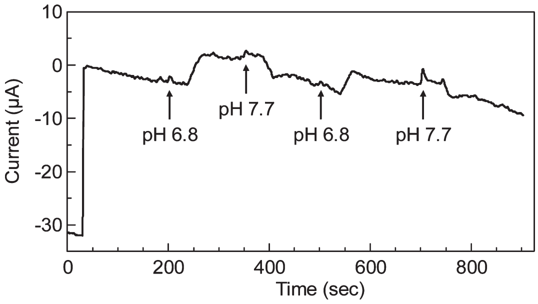

Figure 8. Continuous flow pH sensing by an ODT-passivated InAs/AlSb surface-QW device. Arrows indicate when the pump was switched between the two KH_2PO_4 buffer reservoirs. The delay in current response of ca. 40 s after each pH switch represents the transit time between the buffer reservoir and the sensing chamber. The current was measured by applying an AC bias voltage of 20 mV at 351 Hz between two surface contacts separated by ca. 7.5 mm. The initial sample resistance was 500 Ω. The signal spike at 30 s is a reset offset, and measurements started in pH 7.7 buffer.

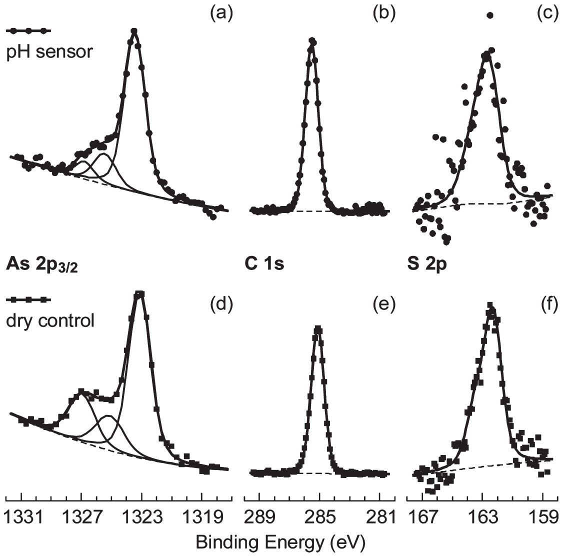

Figure 9. High-resolution elemental XPS data for ODT-passivated InAs/AlSb surface-QW devices. Data in (a−c) are for a device exposed to a flowing KH_2PO_4 solution (circles), and data in (d−f) are for a dry control (squares). Exposing the ODT-passivated device to the phosphate solution did not produce significant oxidation (a versus d) or loss of ODT molecules (c versus f). Symbols = data; thin lines = fit components; dashed lines = backgrounds; thick lines = fit sum curves. For comparison between samples, data are normalized to the intensity of the bulk As 3d component for each sample.

The device exposed to the flowing phosphate solution (Figure 9a−c) shows no catastrophic oxidative degradation; in fact, the As 2p peak shows a smaller As−O_X feature after the solution exposure than that observed for the dry control (Figure 9a, d). The C 1s peak intensity is somewhat higher for the sample exposed to the phosphate solution (Figure 9b, e), but the additional carbon likely originates from sample handling, for example, from the adhesive used for securing the microfluidics chamber. No significant difference is evident between the S 2p peaks for the two samples (Figure 9c, f), which indicates that ODT molecules were not lost from the device surface during the exposure to the flowing phosphate solution and the concomitant surface current measurements.

5. Conclusions

We have demonstrated that a dense monolayer of methyl-terminated alkanethiol molecules can be deposited on InAs(001) surface from a base-activated ethanolic solution held at elevated temperature. We used water CA, XPS, ellipsometry, and electrochemical measurements to characterize the structure and composition of ODT monolayers prepared on InAs. The base-activated deposition procedure effectively removes the native oxide, deposits approximately 1 ML of ODT molecules on InAs(001), and passivates the surface against degradation and reoxidation in air, organic solvents, and in aqueous phosphate buffers (but not in deionized water). The ODT molecules in these monolayers are attached via thiolate bonds almost exclusively to In atoms and organic chains pointing away from the surface.

We have also tested the viability of the base-activated ODT treatment for passivation of InAs/AlSb QW devices and found that the treatment preserves the electronic properties of exposed InAs device surfaces and successfully protects them during electrochemical and continuous flow pH-sensing experiments in aqueous phosphate buffers.

We find that the chemical and electronic passivation of InAs surfaces provided by the base-activated ODT treatment compares favorably—qualitatively and quantitatively—to the results achieved by passivation of related III–V semiconductor surfaces using other inorganic and organic sulfur compounds. The demonstrated compatibility of ODT-passivated InAs devices with realistic measurements in solution indicates that the deposition method described in this work will be useful for developing biosensors and in other practical applications.

Acknowledgment. The authors thank Dr. Cy R. Tamanaha (NRL) and Michael Malito (Nova Research, Inc.) for providing the microfluidics setup; Dr. Kendra M. McCoy (NRL) for assistance with electrochemical measurements; Dr. James C. Culbertson, Dr. F. Keith Perkins, and Dr. Eric S. Snow (NRL) for providing the QW devices and for assistance with electronic and sensor measurements. D.Y.P. thanks Dr. Christine L. McGuiness (The Pennsylvania State University) for insightful discussions of surface chemistry and SAMs on III–V semiconductors. R.S. is an employee of Nova Research, Inc., Alexandria, VA. Funding for this work was provided by the Office of Naval Research and the Air Force Office of Scientific Research.